

One-pot multiphosphinylation & -phosphonylation of pyridine and related heterocycles towards the synthesis of piperidinylphosphonates and -phosphine oxides

Andreas Simoens,^a Prakhar Pouranick,^b Eli Bonneure,^a Johan Sarazin,^c Józef Drabowicz,^{d,e} Guy Van Assche,^b and Christian V. Stevens^{a,*}

^aDepartment of Green Chemistry and Technology, Ghent University, Coupure Links 653, 9000, Ghent, Belgium

^bFaculty of Engineering, Materials and Chemistry, Vrije Universiteit Brussel, Pleinlaan 2, 1050, Brussel, Belgium

^cUnité Matériaux et Transformations – UMR CNRS 8207, Université de Lille, 5900, Lille, France

^dDivision of Organic Chemistry, Center of Molecular and Macromolecular Studies, Polish Academy of Sciences, Sienkiewicza 112, 90-363 Lodz, Poland

^eDepartment of Chemistry, Jan Dlugosz University in Czestochowa, Armii Krajowej 13/15, 42-200 Czestochowa, Poland

Email: Chris.Stevens@UGent.be

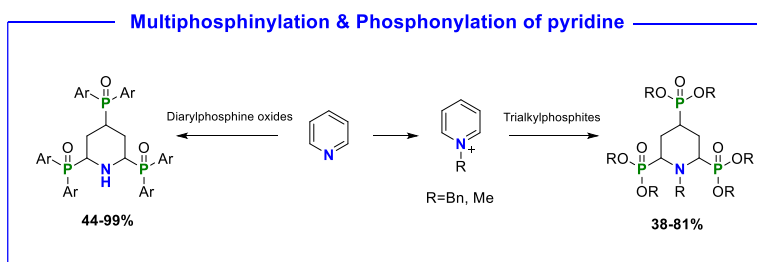
Received 07-19-2024

Accepted 08-28-2024

Published on line 09-15-2024

Abstract

Herein a new protocol for the multiphosphinylation and -phosphonylation of pyridine and related heterocycles is described to give access to piperidinyl phosphine oxides and – phosphonates. The former are accessible through a straightforward, neat, one-pot reaction which yielded the desired phosphinylated heterocycles in moderate to excellent yields (42-99%). These compounds contain a high phosphorus to carbon ratio and were evaluated using TGA and calorimetric measurements for potential flame-retardant applications. The respective phosphonates could be obtained using a second protocol, which employed pyridinium salts, trialkyl phosphites, formic acid and silica to promote the reaction. These piperidinyl phosphonates were isolated in moderate to good yields (38-81%) and provide also an interesting starting point for potential enzyme inhibitors.



Keywords: Phosphonylation, phosphinylation, pyridine, piperidine, flame retardants, phosphine oxides, phosphonates

Introduction

Azaheterocyclic phosphonates are a broad family of compounds that have a widespread use in various fields such as the agrochemical (e.g. Ethephon¹, Roundup²), synthetic and medicinal chemistry field (tenofovir, disoproxil³). The search for new synthetic protocols to synthesize this class of compounds is therefore always active. Some of the most well-known methods for the formation of carbon-phosphorus bonds such as Michaelis-Arbuzov, Michaelis-Becker, Pudovik, Hirao coupling and Kabachnik-Fields reaction, have been around for years and researchers have continuously strived to make them more sustainable and effective.⁴⁻¹³

Phosphonates and phosphine oxides in general are characterized by a stable carbon-phosphorus bond, which can withstand biochemical, thermal and photochemical decomposition.¹⁴ These compounds as well as their respective phosphonic acids can be found in a range of industrial products such as chelating agents,¹⁵ personal care products,¹⁶ detergents,¹⁷ scale inhibitors,¹⁸ flame retardants¹⁹ and water treatment additives.²⁰ Apart from these technical applications, several interesting bioactivities have been accredited to these structures which is often based on their likeness compared to amino acids. The so called α -aminophosphonates and their corresponding acids are structural analogues of natural amino acids and their tetrahedral structure closely resembles the transition state observed during peptide hydrolysis and, as a consequence, these mimics are capable of effectively inhibiting the enzyme's activity.²¹⁻²³

In literature, a number of privileged six-membered azaheterocyclic scaffolds such as pyridine, quinoline, tetrahydroquinoline (THQ) and piperidine have been recognized as interesting targets for the aforementioned phosphorylation reactions and the enzyme inhibiting capabilities of the resulting products have been well-documented.^{10,24,25,29} Especially dominant in current synthetic research are the tetrahydroquinolines (THQs), these motifs are often found in natural products and are linked to a plethora of bioactivities such as antibacterial,²⁸ antiviral,²⁸ antitumor,²⁶ anticoagulant, anti-inflammatory, anti-Parkinson,²⁷ which has resulted in the presence of the THQ skeleton in numerous regulatory approved drugs over the years.²⁹ Previous work performed in our group¹¹ and others³³⁻³⁵ have identified suitable ways of installing phosphorus groups on the quinoline and/or tetrahydroquinoline scaffold.

Additional azaheterocyclic motifs which are plentiful in nature are pyridine and piperidine. While often encountered within bioactive molecules and by themselves considered as important building blocks, it would be highly interesting to evaluate if a straightforward phosphorylation of these structures can be achieved. However, when applying the methods previously successful for the phosphorylation of unprotected quinoline or phenanthroline, it was found that these protocols were incapable of achieving the desired transformation.³⁰⁻³⁵ This prompted us to pursue suitable reaction conditions that would allow to obtain multiphosphorylated piperidine phosphonates and phosphine oxides as well as related heterocycles. Finally, we evaluated if these new structures, prepared with cheap and readily available reagents, would have potential as flame retardants, keeping in mind the known potential of phosphorus and piperidine containing chemicals in this field.

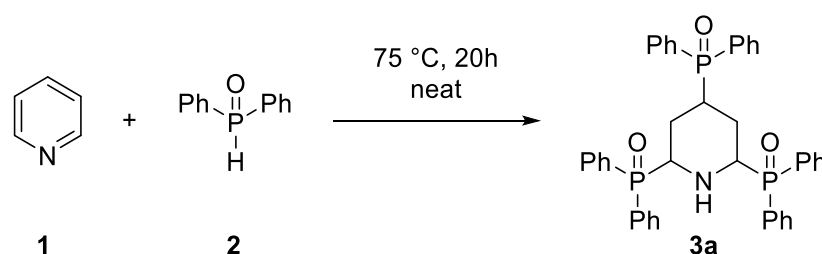
Results and Discussion

Synthesis of piperidinylphosphine oxides

While searching for a suitable protocol to multiphosphorylate the pyridine ring structure in a single step, several literature methods were evaluated. The phosphorylation of (un)protected pyridines towards piperidine phosphonates proved to be impossible with previous methods developed at our group using

silylated phosphite reagents or trialkylphosphites in the presence of acids. Although these more nucleophilic phosphorus compounds proved effective for heterocycles such as quinolines or phenanthrolines,³⁰⁻³² the unreactive pyridine ring remained unaffected. Interestingly, Trofimov et al.³⁵ recently reported the diphosphinylation of unprotected (iso)quinolines using a catalyst free protocol to obtain tetrahydro(iso)quinolines bearing two phosphine oxide groups. After employing an adapted protocol on the pyridine ring structure with commercially available diphenyl phosphine oxide, we were pleasantly surprised when the triphosphonylated product **3a** was readily formed and precipitated from the reaction mixture. Subsequent optimization of the phosphorus reagent equivalents, eventually led to satisfactory yields (Table 1, entry 3). The reaction proceeds without solvent or need for protective atmosphere and the purification step consist of simply washing the solid product with cold acetone, since the desired product proved to have a very low solubility in this solvent, whereas the starting materials are well soluble in acetone.

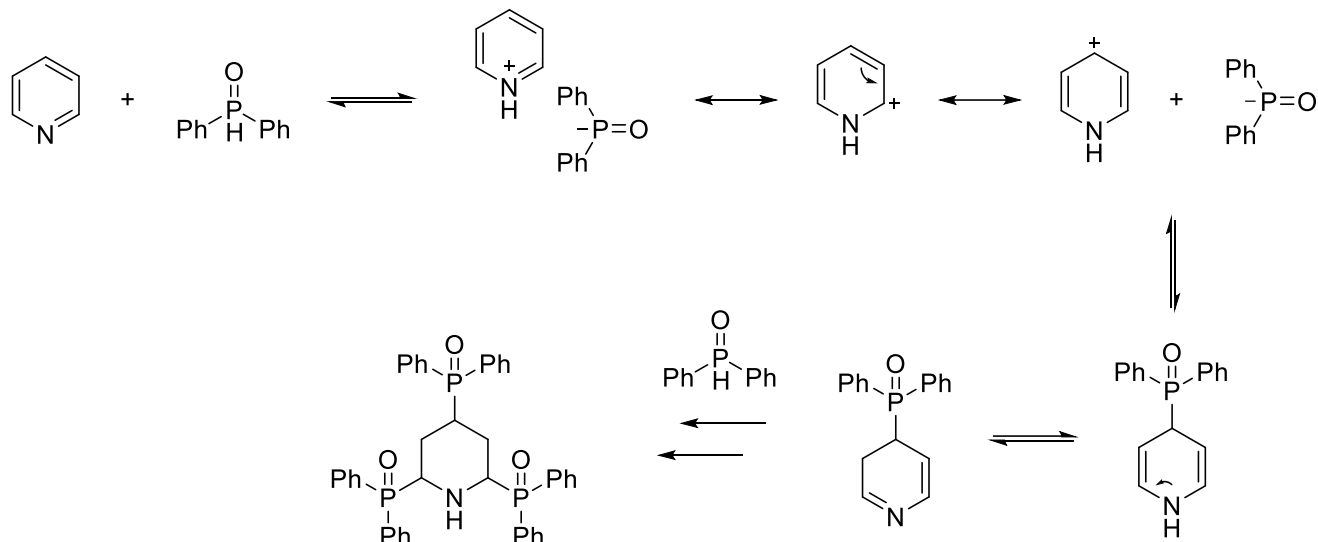
Table 1. Optimization of the synthesis of piperidinyolphosphine oxide



Entry	DPPO	Time (h)	Yield (%)
1	3 eq.	20	55
2	3 eq.	48	53
3	4 eq.	20	82
4	5 eq.	20	80
5	4 eq.	48	75*

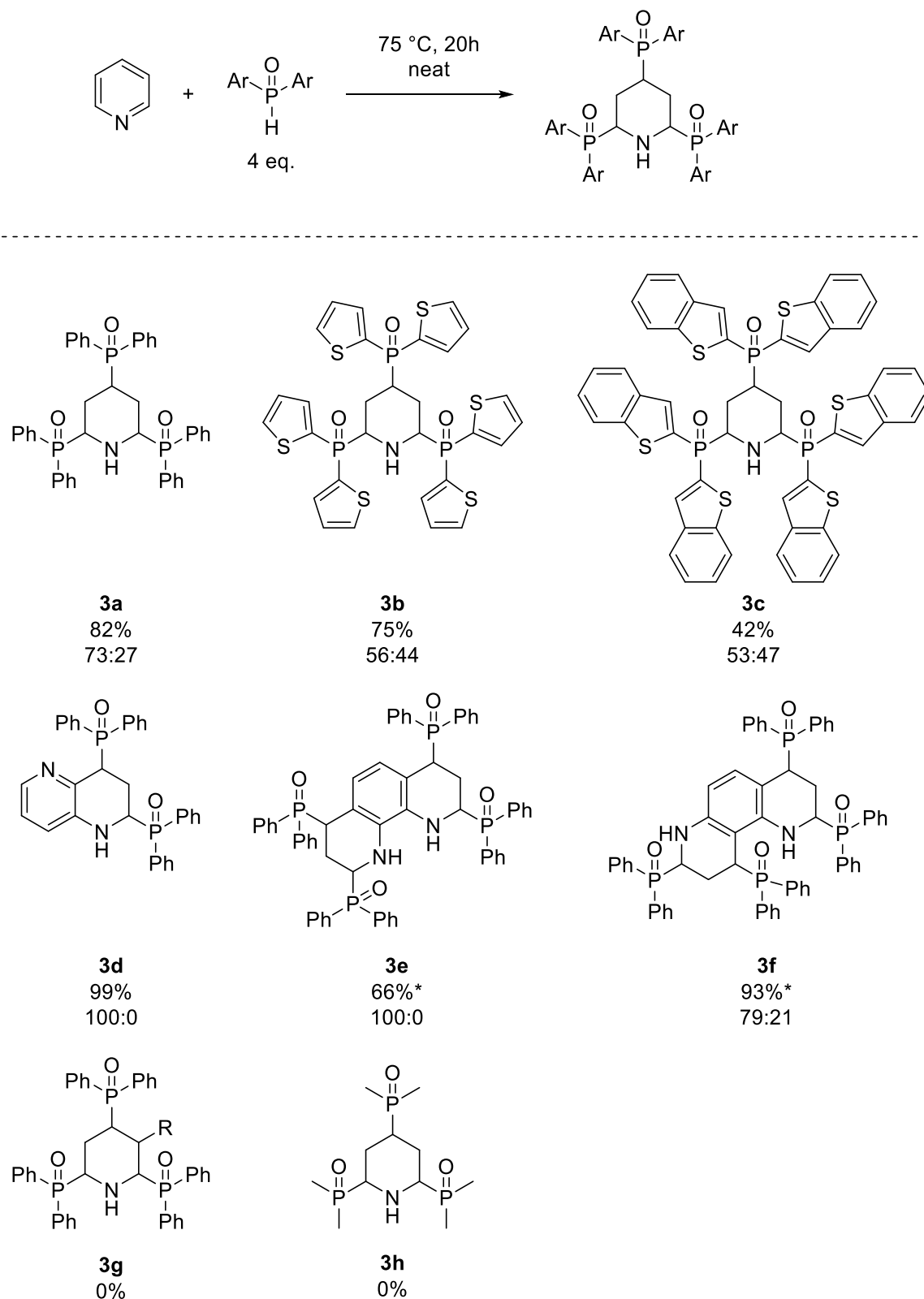
*Large scale reaction: 15.9 g product.

A tentative mechanism for this reaction is presented in scheme 1, based on a similar procedure proposed by Trofimov.³⁵ The sequence starts with a reversible protonation of the pyridine ring by a secondary phosphine oxide to generate an intermediate ion pair, which is further converted to the covalently bound monoadduct. However, this monoadduct is formed reversibly and is, in itself, unstable due to its backward aromatization to pyridine. Upon addition of the second molecule of phosphine oxide, the whole process becomes stabilized because any elimination of phosphine oxide molecules from the piperidine ring does no longer release an aromatic system. The sequence repeats itself until three phosphorus groups are attached.



Scheme 1. Proposed mechanism for the synthesis of piperidinylphosphine oxides.

To explore the scope of this reaction further, a number of less conventional phosphine oxides were synthesized by treating diethyl phosphite with the corresponding Grignard reagents. The compounds bearing aromatic substituents also proved capable of performing the transformation. Unfortunately, when 3-substituted pyridines were used as substrates, none of these pyridine derivatives were susceptible to the reaction conditions. This is most likely due to steric hindrance towards the addition of these bulky phosphorus reagents, as both electron donating and withdrawing groups were evaluated and did not lead to the desired end products. Larger ring systems such as phenanthrolines **3e** & **3f** could also be used, adding 4 phosphine oxide moieties to the structure. This is interesting because the previously developed method in our group for the phosphonylation of these structures (with less stable dialkyl trimethylsilyl phosphite), was only capable of adding two phosphorus moieties. This follows directly from the need of an acid activation of the aromatic nitrogen atom, which was rendered impossible after the first 1,4-1,2-addition.³⁰ Finally, when 1,5-naphthyridine was reacted with 4 equivalents of diphenyl phosphine oxide (**3d**), we noticed only a diphosphonylation took place regardless of the larger excess of reagent. The smaller size of this structure compared to the aforementioned phenanthrolines most likely causes too much steric hindrance, preventing the nucleophilic attack of the third and fourth phosphine oxide. For the successfully obtained structures, multiple diastereomers were observed in the ³¹P NMR spectrum of which the ratios are given in Figure 1.



R = OMe, F, Cl, Ac

*5 equiv. diphenylphosphine oxide used, reaction time 48 hours.

Figure 1. Evaluating the scope of the phosphinylation reaction using phosphine oxides.

When analysing the product mixtures it became evident that for several of the target compounds multiple diastereomers were present. The major product was deduced to be **3a(Major)**. This was supported by the fact that the proton ($N\text{-CH-P}$) and phosphorus atoms adjacent to the nitrogen atom, presented themselves on NMR at identical shifts which implied symmetry for these nuclei in the molecule. On the other hand, the **3a(Minor)** product did not present any interaction for these protons in the NOESY spectrum and because of the lack of symmetry in this diastereomer, the ^1H & ^{31}P NMR signals were now observed as separate signals. Further the phosphorus in the para position is coupling with one of the ortho phosphorus groups, being on the same face of the ring (Figure 2). These arguments also held true for the other piperidine analogues and the characterization data of these compounds can be found in the supporting information.

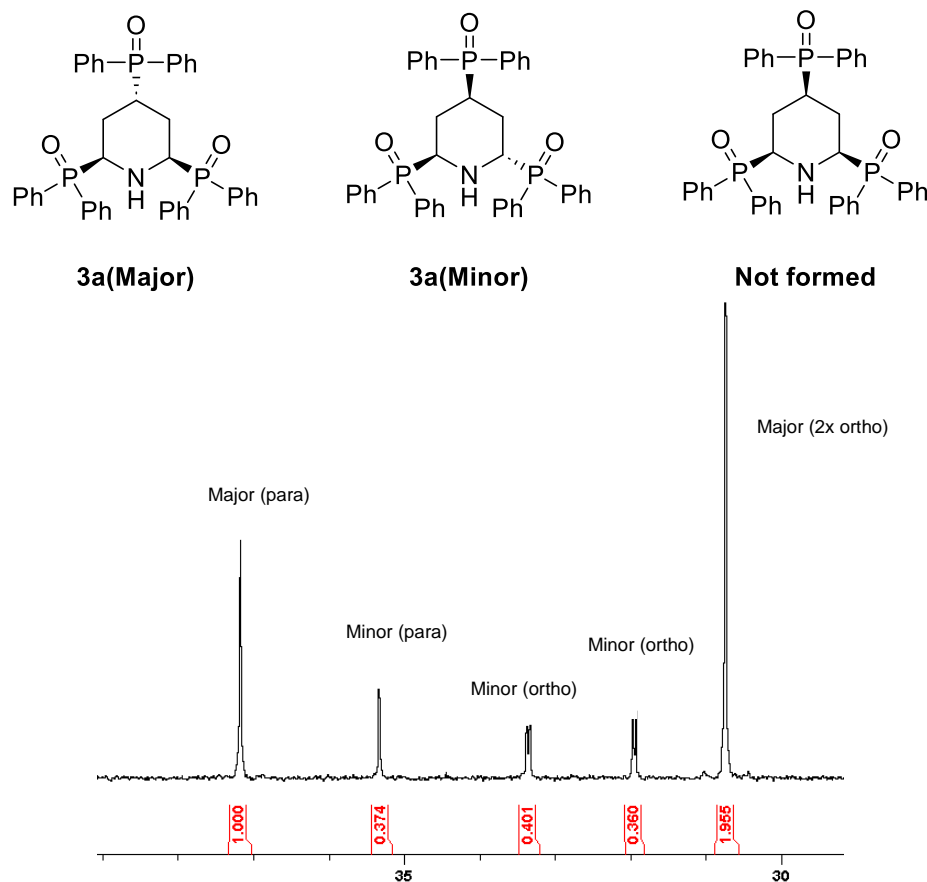


Figure 2. Possible major and minor diastereomers present in the phosphine oxide mixture and the corresponding ^{31}P -NMR.

Given the ease of this protocol and the low cost of the used chemicals, we opted to demonstrate that a large-scale synthesis of the model compound was possible. After a successful large-scale reaction (15.9 g, 75%) and with a sizeable amount of this compound in hand, we were curious to evaluate the flame-retardant properties of this molecule. It has long been known that phosphorus rich chemicals are of great interest in this field¹⁹ and even the piperidine core structure has been found to possess a radical quenching effect in the gaseous phase, further contributing to the potential flame retardancy of this compound.³⁶⁻⁴¹ The main techniques used in this work are thermogravimetric analysis (TGA) and pyrolysis combustion flow calorimetry (PCFC). TGA is used to study the thermal stability of the prepared structures in air (Figure 3) and inert N_2

(Figure 4) atmosphere. PCFC is utilised to study the fire behaviour of these materials (Figure 5). Large scale cone calorimetry was not used due to the lower amount of sample availability for some derivatives.

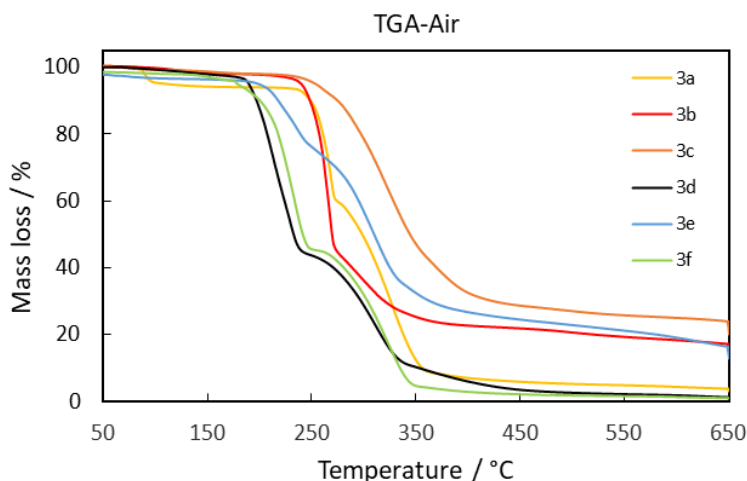


Figure 3. TGA measurements for the obtained structures in air.

Measurements in air (Figure 3) showed that for structure **3c** the temperature at the onset of degradation $T_{5\%}$ (mass loss of 5 wt.% of the initial mass) was the highest at 253 °C, followed by **3b** at 241 °C. Compound **3a** showed the earliest start of degradation of all structures at 110 °C. The higher this initial degradation temperature ($T_{5\%}$) is, the higher the initial thermal stability of the material. Comparing the amount of residue/char formed after degradation, **3c** formed the highest amount of residue with 20 wt% at 650 °C, followed by **3b** with 15 wt% residue and **3e** with 13 wt% residue. All other structures showed char/residue below 5 wt%. The char/residue that is formed during the degradation process can act as a protective layer on the material and slow down further thermal degradation of the material.

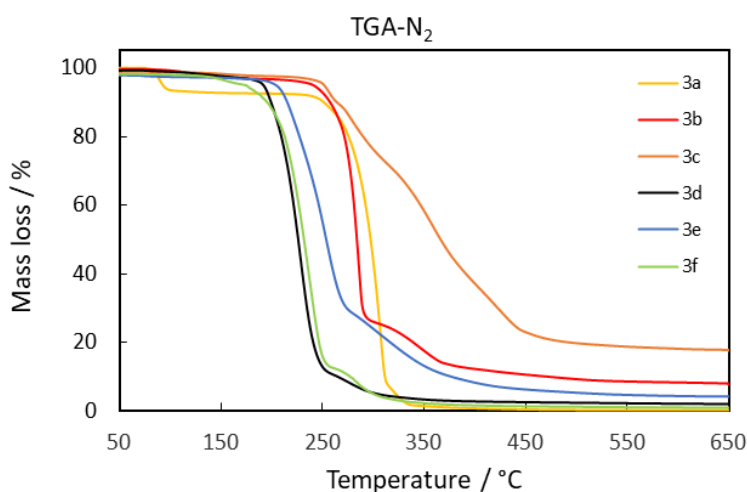


Figure 4. TGA measurements for the obtained structures under N₂ atmosphere.

Measurements in N₂ also showed similar trends (Figure 4) with **3c** showing the highest thermal stability at the start of degradation, $T_{5\%}$ at 251 °C and the highest amount of char formed at 17 wt.%. Similarly to air, **3b**

also showed the second highest thermal stability at the start of degradation, $T_{5\%}$ at 242 °C and also the second highest char formation at 8 wt%. **3a** again showed the lowest thermal stability with degradation starting at 93 °C. All other structures showed char formation below 5 wt%. For structure **3a**, TGA measurements in both air and N_2 must be taken with caution because this initial mass loss might be due to moisture present in the sample (yellow curve in Figure 3 and Figure 4), its degradation curve stabilised after that point, making it more thermally stable than **3d** and **3f**.

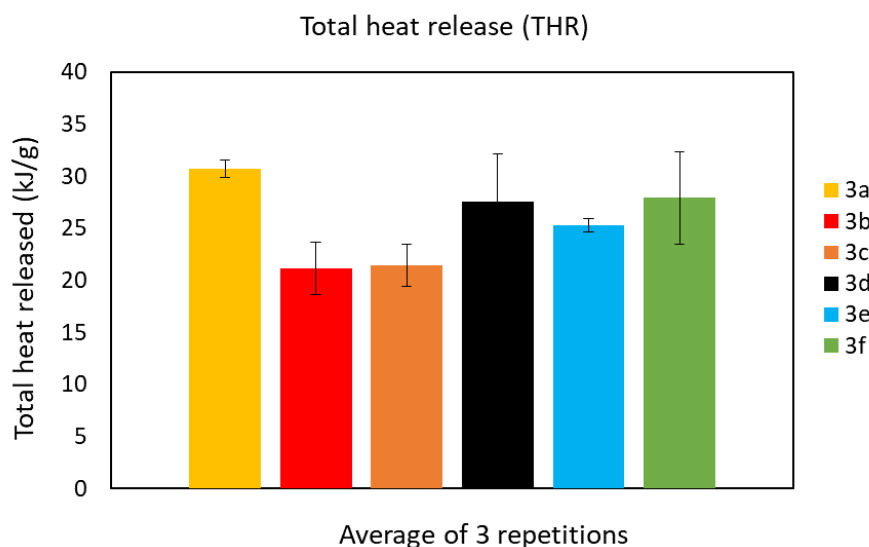


Figure 5. PCFC measurements and their obtained total heat release.

Table 2. Total heat release values in kJ.g^{-1} for the synthesized phosphine oxides

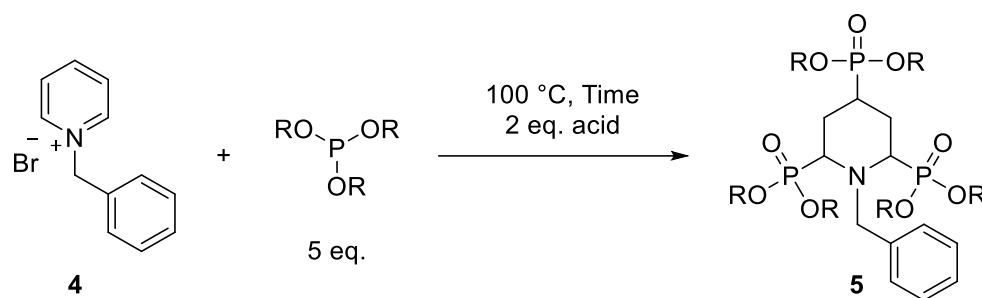
Sample	Total HR (kJ.g^{-1})
3a	30.73±0.85
3b	21.15±2.49
3c	21.45±2.03
3d	27.54±4.59
3e	25.30±0.64
3f	27.92±4.44

The total heat released was found to be the lowest for **3b** and **3c** in the PCFC measurements, at $21.15 \pm 2.49 \text{ kJ.g}^{-1}$ and $21.45 \pm 2.03 \text{ kJ.g}^{-1}$, respectively. The highest value for the total heat released was observed for **3a**, at $30.73 \pm 0.85 \text{ kJ.g}^{-1}$. With regard to fire behaviour, **3b** and **3c** exhibited the most favourable characteristics, and also displayed the highest thermal stability. To make an accurate assessment of the flame retardant potential of these materials, a next step will be to incorporate the most promising candidates as an additive into a polymer system and evaluate their effect on the thermal stability and the heat released during combustion of this material.

Synthesis of piperidinyolphosphonates

When attempting to use the same method for the synthesis of piperidine phosphonates, it turned out that these reactions conditions were not suitable and a different protocol had to be optimized. Initially, an acid

activated phosphorylation using dialkyl trimethylsilyl phosphite was attempted unsuccessfully. The unreactivity of the pyridine ring, gradual hydrolysis of the phosphorus reagent and two-phase mixing problems are the cause of this failure. The combination of sulphuric acid with pyridine leads to the formation of an ionic liquid which is generally known to be quite stable and proved to be immiscible with the reagent.⁴² After evaluating a number of acids (H_2SO_4 , HCl, formic acid and methanesulfonic acid), phosphorus reagents (triethyl phosphite, dimethyl trimethylsilylphosphite, diethyl trimethylsilylphosphite) and different solvents, there were no hopeful results that suggested this transformation would be successful on an unprotected (acid activated) pyridine ring. This made us shift our attention to the use of pyridinium salts as a substrate, as this would remedy the ionic liquid formation and help with the reactivity of the pyridine ring. N-benzylpyridinium bromide could easily be made in high yields (92-98%) using known literature methods.⁴³ Exposing this compound to the silylated phosphite reagent under reflux conditions gave us the first sign of di- and triphosphonylated product, and after 3 days about 45% conversion was reached (Table 3, entry 1). In an attempt to further optimize these conditions, a protective atmosphere and carefully dried reagents were used to carry out the reaction to avoid excessive hydrolysis of the phosphorus reagents. No reaction occurred when using dialkyl phosphites, so hydrolysis towards these compounds had to be avoided as much as possible. Upon realizing that the reaction also took place using the more stable and commercially available triethyl phosphite (Table 3, entry 2), this reagent was chosen for further optimization of the reaction. Considering the need for additional protons within the final product, we explored the possibility of adding an additional acid to the mixture hoping to boost the conversion. While the use of H_2SO_4 and methanesulfonic acid only lead towards full hydrolysis of the triethyl phosphite present, formic acid was capable of fully converting the starting product after three days at 100 °C, as observed on ^{31}P -NMR (Table 3, entry 6). Not yet completely satisfied with these results, we explored the possibility of using an additional additive to speed up the reaction, as well as the selectivity towards the triphosphonylated product. A previous article by Lavilla et al. described the oxidative diphosphonylation of substituted pyridinium salts. In this work they found that one of the phosphonate groups would move from the ortho- to the more stable para-position upon contact with SiO_2 .⁴⁴ This prompted us to add a catalytic amount (10 wt%) of silica to the mixture, which further increased the reaction speed and selectivity (Table 3, entry 7). Using microwave heating for this protocol was also possible and allowed for a full conversion after 4 hours (Table 3, entry 8).

Table 3. Optimization of the synthesis of piperidinylphosphonates

Entry	Phosphite reagent	Time (h)	acid	Conv (%)
1	DEPTMS	72	/	45
2	Triethyl phosphite	72	/	28
3	Diethyl phosphite	72	/	0
4	Triethyl phosphite	72	H ₂ SO ₄	Hydrolysis
5	Triethyl phosphite	72	CH ₃ SO ₃ H	Hydrolysis
6	Triethyl phosphite	72	HCOOH	100
7	Triethyl phosphite	24	HCOOH	100*
8	Triethyl phosphite	4	HCOOH	100**

*10 wt% SiO₂ added.

**MW heating + use of 10 wt% SiO₂.

To illustrate the importance of the acid and the silica additive, Figure 6 shows the comparison of the respective conversion towards tri- or diphosphonylated product after 1 day of reaction using the different catalytic systems under conventional heating.





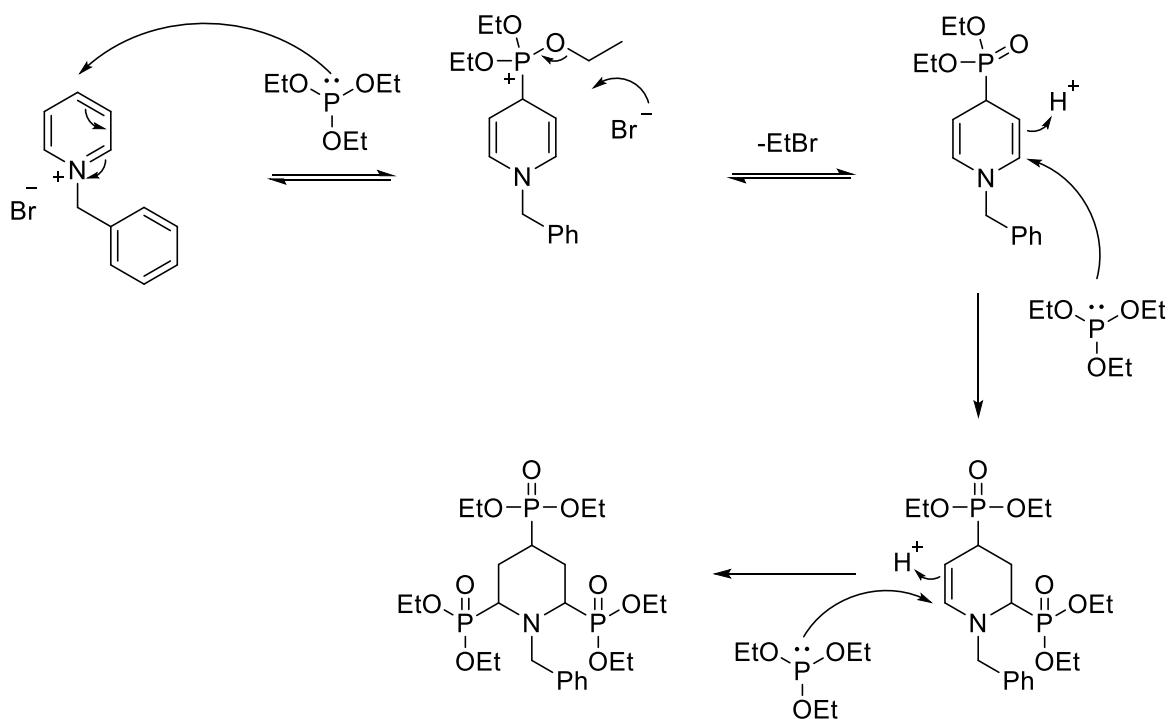
	<i>NMR yield after 24 h</i>	3P	2P	
Formic acid, SiO ₂		100%	96%	4%
Formic acid		65%	46%	19%
SiO ₂		7%	7%	-
No additives		9%	8%	1%

Figure 6. Influence of the additives on the conversion towards phosphonylated products.

In Scheme 2, a plausible mechanism for this acid catalyzed phosphonylation is presented. The reaction begins with the addition of a nucleophilic trivalent phosphite agent at the more accessible para-position. By interaction with a nucleophile, such as the bromide counter anion, a phosphonate group is formed and volatile ethyl bromide is expelled. Next, the second nucleophilic attack of a phosphite species occurs. Since aromaticity was broken in the previous step, this subsequent addition occurs rapidly and is accompanied by the incorporation of a hydrogen atom promoted by the acidic medium. This is repeated a final time to produce the triphosphonylated product.



Scheme 2. Plausible mechanism for the synthesis of piperidinyolphosphonates.

With the optimized conditions in hand, a small library of products was prepared, using different commercially available phosphite reagents (Figure 7). Once again, any substitution of the pyridine core on the 3-position severely hindered the transformation (**5e**). The 2-methylpyridinium salt formed traces of product, but remained mainly stuck at the diphosphonylated product as expected. 4-Methylpyridinium showed no signs of product formation whatsoever, which supports the hypothesis of a 1,4-1,2 addition for this reaction. The quinoline substrate was once again well tolerated (**5f**), but as mentioned earlier, can also be made with

unprotected quinoline using silylated phosphite reagents. The N-methylated piperidine **5d** was obtained in lower yield (38%), mainly due to a difficult purification step required to separate it from remaining diphosphonylated product.

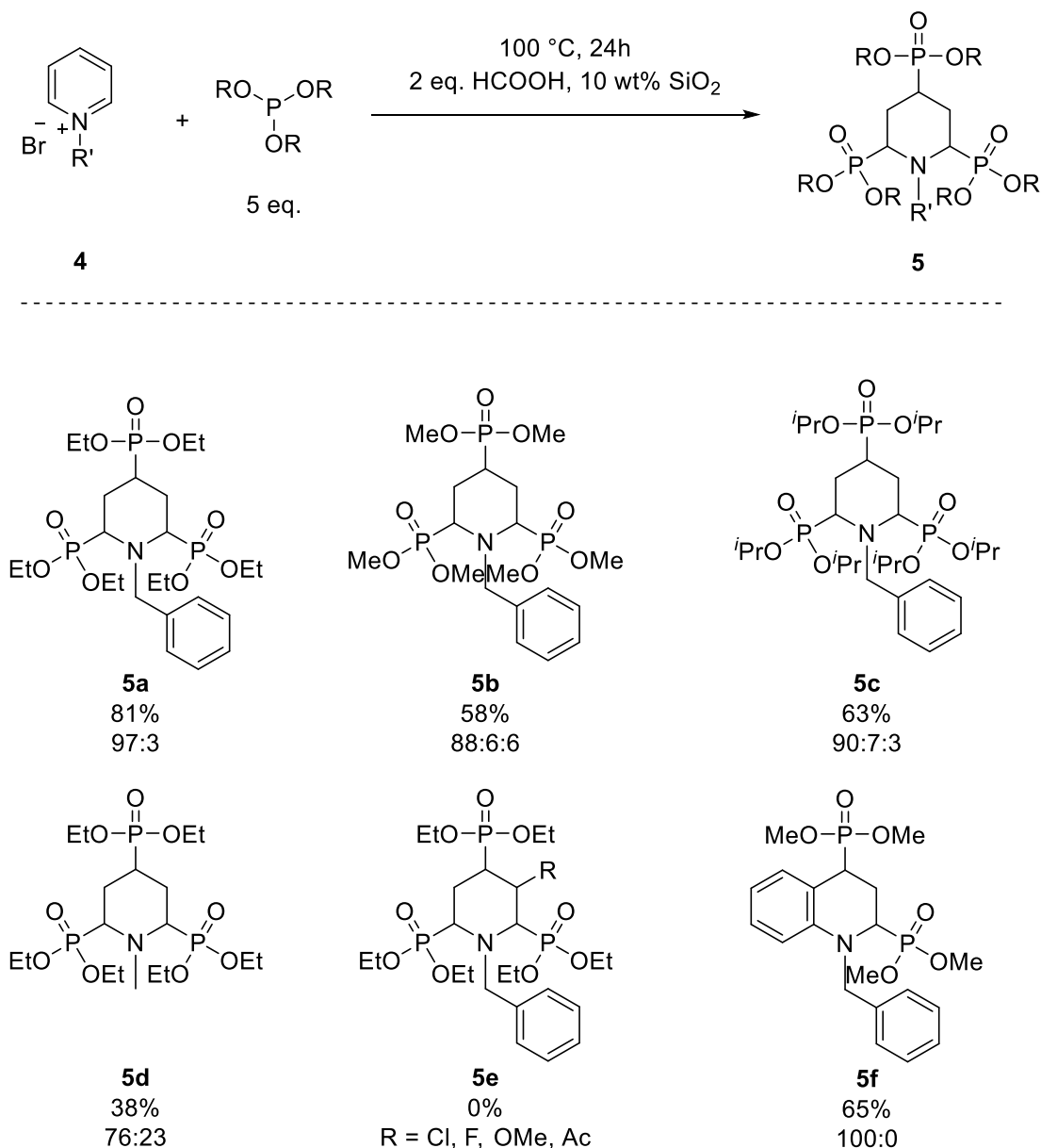


Figure 7. Evaluating the scope of the phosphonylation reaction using trialkylphosphites including the yields and the dr.

Just as for the previous reaction, a combination of diastereomers was often found when analysing these mixtures. However, for the phosphonates the opposite result seemed to be true. The **5a(Major)** product had no observable spatial interactions for the relevant protons and the major product gave three separate ^{31}P NMR signals as expected for the non-symmetrical molecule (Figure 8). The **5a(Minor)** product, being the symmetrical diastereomer in this case, only presented two signals, with the phosphorus atoms in the ortho position at the exact same chemical shift. This observation once again held true for the other piperidine

derivatives. After chromatography on silica, the mixtures were often enriched with the major compound (as seen in Figure 7) which helped the characterization.

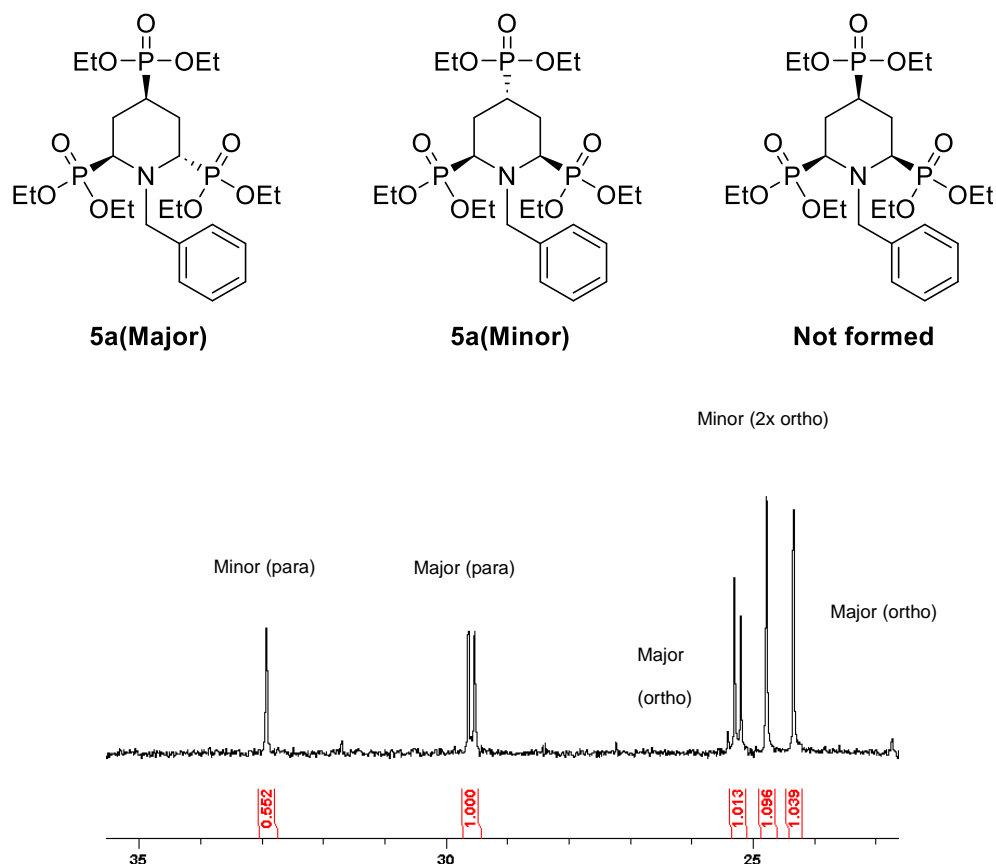


Figure 8. Possible major and minor diastereomers present in the phosphonates mixture (pre-purification).

Conclusions

In summary, we were able to effectively broaden the scope of substrates which are capable of undergoing a multiphosphinylation and -phosphonylation reaction. First, we produced piperidinyll phosphine oxides from unprotected pyridine as well as other heterocycles such as naphthyridine and phenanthroline, through a one-step reaction which requires no additional solvent. These compounds could be easily purified and were subsequently evaluated in TGA and calorimetric measurements, as their high phosphorus and carbon content could prove interesting for flame retardant applications. Next, a suitable protocol to access the piperidinyll phosphonates was targeted and successfully reached through the initial formation of the respective pyridinium salts. By employing a suitable acid catalyst in combination with silica, the envisioned phosphonates could be obtained in moderate to good yields. In each case the most likely major and minor diastereomers were identified.

Experimental Section

Di(thiophen-2-yl)phosphine oxide & di(benzothiophen-2-yl)phosphine oxide. A flame dried flask is filled with a suspension of magnesium turnings (720 mg, 30 mmol) in anhydrous THF (20 mL). To this suspension is then added 2-bromothiophene (0.4 mL, 4 mmol) (or 2-bromobenzothiophene). When the reaction mixture starts to heat up and the Grignard reagent is forming, the remaining 2-bromothiophene/2-bromobenzothiophene (2.5 mL, 26 mmol) in THF (10 mL) is added. After stirring this mixture for 2 hours at room temperature, the flask is cooled to -20 °C using a cooling bath with a NaCl:ice mixture of 1:3 mass ratio. When the contents are sufficiently cooled, diethyl phosphite (1.28 mL, 10 mmol) in THF (10 mL) is added dropwise to the mixture. Next, the cooling bath is removed and the reaction is stirred at room temperature for another 2 hours. To quench the reaction, 0.5 M HCl solution (30 mL) is added dropwise to the mixture, after which the contents are transferred to a separatory funnel. The product is extracted using EtOAc (2 × 30 mL), and the organic phase is subsequently washed with brine. After drying the combined organic fractions with MgSO₄ and filtering off the solids, the desired product is obtained as a yellow oil (89% yield) in the case of the di(thiophen-2-yl) derivative and a beige powder (77% yield) in the case of di(benzothiophen-2-yl) phosphine oxide. The resulting products are pure enough for further use. Adapted from and spectral data in accordance with literature.⁴⁵

Synthesis of piperidynylphosphine oxides (3). A round bottom flask is filled with 0.2 g of pyridine (or phenanthroline/quinazoline) and 4 equivalents of diarylphosphine oxide. After adding a stirring bar, the flask is closed with a rubber septum and the mixture is heated at 75 °C for 20 hours. Initially the phosphorus reagent melts upon heating and creates a liquid and clear mixture. As the reaction reaches its end, the desired product precipitates as a solid. The solid product is broken up with a spatula and acetone is added to dissolve and wash out any remaining starting product. The desired product is collected through filtration to obtain the phosphonylated heterocycles in decent to excellent yields (42-99%).

Synthesis of *N*-benzylpyridinium bromide (4). Pyridine (3.00 mL, 37.2 mmol) was mixed with dichloromethane (6 mL) and benzyl bromide (4.50 mL, 36.6 mmol) in a 50 mL round bottom flask. The mixture was stirred overnight (for 16 h) at 50 °C. The solvent was then evaporated under reduced pressure and the product is washed with diethyl ether. After filtration the remaining ether is evaporated and the product is further dried under high vacuum. The desired compound is obtained as yellow crystals in near quantitative yield.⁴⁶

Synthesis of *N*-methylpyridinium iodide. Trimethylsulphoxonium iodide (1 g, 4.55 mmol) is dissolved in 5 mL of pyridine and refluxed (115 °C) for 15 minutes. Afterwards, the reaction mixture is cooled to room temperature and the produced crystals are removed by filtration. Next, the filtrate is washed with diethyl ether and cold pyridine. This process is repeated 3 times, after which the salt is dried under high vacuum. The final compound (1-methylpyridinium iodide) is a colorless solid (92% yield).⁴⁷

Synthesis of piperidynylphosphonates (5). To a flame dried 10 mL flask under inert atmosphere, 1 mmol of pyridinium salt (250 mg *N*-benzylpyridinium bromide or 221 mg *N*-methylpyridinium iodide) is added along with 0.25 mg of dry silica (10 wt%), 2 equivalents of formic acid (0.08 mL, 2 mmol) and an excess of trialkyl phosphite (5 equivalents, 5 mmol). Afterwards, the flask is flushed again with an inert gas (e.g. nitrogen, argon) and heated at 100 °C for 24 hours. The product is isolated by first removing the remaining phosphite reagent through distillation (95 °C at 13 mPa). The remaining mixture is dissolved in dichloromethane, after which the compound is purified by column chromatography, using a dichloromethane/methanol mixture with a 95/5 ratio. Finally, the product was dried under high vacuum to remove any residual solvent and obtained as an orange oil (38-81% yield).

Supplementary Material

The data underlying this study are available in the published article and its Supporting Information.

References

1. Dahnous, K.; Vigue, G.; Law, A.; Konzak, C.; Miller, D. *Agron. J.* **1982**, *74*, 580-582.
<https://doi.org/10.2134/agronj1982.00021962007400030041x>
2. Smith, E.; Oehme, F. *Vet. Hum. Toxicol.* **1992**, *34*, 531-543.
3. Viread® (tenofovir disoproxil fumarate); Gilead Sciences, Inc., 2024)
https://www.gilead.com/-/media/files/pdfs/medicines/liver-disease/viread/viread_pi.pdf
4. Debrouwer, W.; Wauters, I.; Stevens, C. V. Methods for the Introduction of the Phosphonate Moiety into Complex Organic Molecules. In *Organophosphorus Chemistry: From Molecules to Applications*, Iaroshenko, V. Ed.; Wiley-VCH Verlag GmbH & Co. KGaA, **2019**; p 249.
<https://doi.org/10.1002/9783527672240.ch7>
5. Henyecz, R.; Keglevich, G. *Curr. Org. Synth.* **2019**, *16*, 523-545.
<https://doi.org/10.2174/1570179416666190415110834>
6. Henyecz, R.; Keglevich, G. P-C couplings by the Hirao reaction. In *Organophosphorus Chemistry*, Walter de Gruyter GmbH, **2018**; p 158.
<https://doi.org/10.1515/9783110535839-008>
7. Jablonkai, E.; Keglevich, G. *Curr. Green Chem.* **2015**, *2*, 379-391.
<https://doi.org/10.2174/2213346102999150630114117>
8. Keglevich, G. *Molecules* **2021**, *26*, 1196.
<https://doi.org/10.3390/molecules26041196>
9. Keglevich, G.; Henyecz, R.; Mucsi, Z. *Molecules* **2020**, *25*, 3897.
<https://doi.org/10.3390/molecules25173897>
10. Van der Jeught, S.; Stevens, C. V. *Chem. Rev.* **2009**, *109*, 2672-2702.
<https://doi.org/10.1021/cr800315j>
11. Budnikova, Y. H.; Gryaznova, T. V.; Grinenko, V. V.; Dudkina, Y. B.; Khrizanforov, M. N. *Pure Appl. Chem.* **2017**, *89*, 311-330.
<https://doi.org/10.1515/pac-2016-1001>
12. Luo, K.; Yang, W.-C.; Wu, L. *Asian J. Org. Chem.* **2017**, *6*, 350-367.
<https://doi.org/10.1002/ajoc.201600512>
13. Mayorquin-Torres, M. C.; Simoens, A.; Bonneure, E.; Stevens, C. V.; *Chem. Rev.* **2024**, *124*, 7907-7975.
<https://doi.org/10.1021/acs.chemrev.4c00090>
14. Kafarski, P. Biological Role of Phosphorus; IntechOpen, **2019**.
15. Maier, L.; Crutchfield, M. M. *Phosphorus, Sulfur Relat. Elem.* **1978**, *5*, 45.
<https://doi.org/10.1080/03086647808069861>
16. Carella, F.; Esposti, L. D.; Adamiano, A.; Iafisco, M. *Materials (Basel)* **2021**, *14*, 6398.
<https://doi.org/10.3390/ma14216398>
17. Gledhill, W. E.; Feijtel, T. C. *The Handbook of Environmental Chemistry: Detergents*; Springer, **1992**, 261-285.
https://doi.org/10.1007/978-3-540-47108-0_8

18. Lu, H.; McCabe, B.; Brooks, J.; Heath, S.; Stevens, S. *SPE International Conference on Oilfield Chemistry*, **2019**.
<https://doi.org/10.1016/j.chemosphere.2012.03.067>
19. van der Veen, I.; de Boer, J. *Chemosphere* **2012**, *88*, 1119-1153.
20. Rosales, E.; Del Olmo, G.; Preciado, C. C.; Douterelo, I. *Front. Microbiol.* **2020**, *11*, 599091.
<https://doi.org/10.3389/fmicb.2020.599091>
21. Hoerlein, G. *Rev. Environ. Contam. Toxicol.* **1994**, *138*, 73-145.
<https://doi.org/10.2174/0929867311320160004>
22. Tusek-Bozic, L. *Curr. Med. Chem.* **2013**, *20*, 2096-2117.
<https://doi.org/10.2174/0929867311320160004>
23. Sienczyk, M.; Oleksyszyn, J. *Curr. Med. Chem.* **2009**, *16*, 1673-1687.
<https://doi.org/10.2174/092986709788186246>
24. Cui, P.-C.; Yin, Z.-C.; Wang, G.-W. *Org. Lett.* **2023**, *25*, 2663-2668.
<https://doi.org/10.1021/acs.orglett.3c00738>
25. Gusarova, N. K.; Volkov, P. A.; Ivanova, N. I.; Arbuzova, S. N.; Khrapova, K. O.; Albanov, A. I.; Smirnov, V. I.; Borodina, T. N.; Trofimov, B. A. *Tetrahedron Lett.* **2015**, *56*, 4804-4806.
<https://doi.org/10.1016/j.tetlet.2015.06.062>
26. Scott, J. D.; Williams, R. M. *Chem. Rev.* **2002**, *102*, 1669-1730.
<https://doi.org/10.1021/cr010212u>
27. Vetulani, J.; Antkiewicz-Michaluk, L.; Nalepa, I.; Sansone, M. *Neurotoxic. Res.* **2003**, *5*, 147-155.
<https://doi.org/10.1007/BF03033379>
28. Singh, I. P.; Shah, P. *Expert Opin. Ther. Pat.* **2017**, *27*, 17-36.
<https://doi.org/10.1080/13543776.2017.1236084>
29. Kim, A. N.; Ngamnithiporn, A.; Du, E.; Stoltz, B. M. *Chem. Rev.* **2023**, *123*, 9447-9496.
<https://doi.org/10.1021/acs.chemrev.3c00054>
30. De Blicck, A.; Catak, S.; Debrouwer, W.; Drabowicz, J.; Hemelsoet, K.; Verstraelen, T.; Waroquier, M.; Van Speybroeck, V.; Stevens, C. V. *Eur. J. Org. Chem.* **2013**, 1058-1067.
<https://doi.org/10.1002/ejoc.201201437>
31. De Blicck, A.; Masschelein, K. G. R.; Dhaene, F.; Rozycka-Sokolowska, E.; Marciniak, B.; Drabowicz, J.; Stevens, C. V. *Chem. Commun.* **2010**, *46*, 258-260.
<https://doi.org/10.1039/B906808B>
32. Van Waes, F. E. A.; Debrouwer, W.; Heugebaert, T. S. A.; Stevens, C. V. *Arkivoc* **2014**, *i*, 386-427.
<https://doi.org/10.3998/ark.5550190.p008.648>
33. Zhang, Q.; Wei, D.; Cui, X.; Zhang, D.; Wang, H.; Wu, Y. *Tetrahedron* **2015**, *71*, 6087-6093.
<https://doi.org/10.1016/j.tet.2015.07.001>
34. Gao, Y.; Deng, H.; Zhang, S.; Xue, W.; Wu, Y.; Qiao, H.; Xu, P.; Zhao, Y. *J. Org. Chem.* **2015**, *80*, 1192-1199.
<https://doi.org/10.1021/jo501842p>
35. Trofimov, B. A.; Volkov, P. A.; Telezhkin, A. A.; Khrapova, K. O.; Ivanova, N. I.; Albanov, A. I.; Gusarova, N. K. *J. Org. Chem.* **2020**, *85*, 4927-4936.
<https://doi.org/10.1021/acs.joc.0c00084>
36. Huo, S.; Wang, J.; Yang, S.; Zhang, B.; Chen, X.; Wu, Q.; Yang, L. *Polym. Degrad. Stab.* **2017**, *146*, 250-259.
<https://doi.org/10.1016/j.polymdegradstab.2017.10.015>
37. Xie, H.; Lai, X.; Li, H.; Zeng, X. *Polym. Degrad. Stab.* **2016**, *130*, 68-77.
<https://doi.org/10.1016/j.polymdegradstab.2017.10.015>

38. Aubert, M.; Wilén, C.-E.; Pfaendner, R.; Kniesel, S.; Hoppe, H.; Roth, M. *Polym. Degrad. Stab.* **2011**, *96*, 328-333.
<https://doi.org/10.1016/j.polymdegradstab.2010.02.035>
39. Lai, X.; Qiu, J.; Li, H.; Zhou, R.; Xie, H.; Zeng, X. *J. Anal. Appl. Pyrol.* **2016**, *120*, 361-370.
<https://doi.org/10.1016/j.jaap.2016.06.004>
40. Cao, K.; Wu, S.-L.; Qiu, S.-L.; Li, Y.; Yao, Z. *Ind. Eng. Chem. Res.* **2013**, *52*, 309-317.
41. Marney, D. C. O.; Russel, L. J.; Stark, T. M. *Polym. Degrad. Stab.* **2008**, *93*, 714-722.
<https://doi.org/10.1016/j.polymdegradstab.2007.12.008>
42. Freemantle, M. *An introduction to ionic liquids*; Royal Society of Chemistry, **2010**.
<https://doi.org/10.1039/9781839168604>
43. Sowmiah, S.; Esperanca, J. M. S. S.; Rebelo, L. P. N.; Afonso, C. A. M. *Org. Chem. Front.* **2018**, *5*, 453-493.
<https://doi.org/10.1039/C7QO00836H>
44. Lavilla, R.; Spada, A.; Bosch, J. *Org. Lett.* **2000**, *2*, 1533-1535.
<https://doi.org/10.1021/ol0057380>
45. Hao, Y.; Wu, D.; Tian, R.; Duan, Z.; Mathey, F. *Dalton Trans.* **2016**, *45*, 891-893.
<https://doi.org/10.1039/C5DT04245C>
46. Jensen, A. W.; Moore, J. M.; Kimble, M. V.; Ausmus, A. P.; Dilling, W. L. *Tetrahedron Lett.* **2016**, *57*, 5636-5638.
<https://doi.org/10.1016/j.tetlet.2016.11.013>
47. Kuhn, R.; Trischmann, H. *Liebigs Ann. Chem.* **1958**, *611*, 117-121.
<https://doi.org/10.1002/jlac.19586110112>

This paper is an open access article distributed under the terms of the Creative Commons Attribution (CC BY) license (<http://creativecommons.org/licenses/by/4.0/>)